Ecological Applications, 16(3), 2006, pp. 1148–1163

RECOVERY OF FOREST STRUCTURE AND SPECTRAL PROPERTIES AFTER SELECTIVE LOGGING IN LOWLAND BOLIVIA

Eben N. Broadbent,[1,2] Daniel J. Zarin,[1,5] Gregory P. Asner,[2] Marielos Peña-Claros,[3] Amanda Cooper,[2] and Ramon Littell[4]

[1]*School of Forest Resources and Conservation, University of Florida, Gainesville, Florida, 32611 USA*
[2]*Department of Global Ecology, Carnegie Institution, 260 Panama Street, Stanford, California, 94305 USA*
[3]*Instituto Boliviano de Investigación Forestal, Casilla 3632, Santa Cruz, Bolivia*
[4]*Department of Statistics, University of Florida, Gainesville, Florida, 32611 USA*

Abstract. Effective monitoring of selective logging from remotely sensed data requires an understanding of the spatial and temporal thresholds that constrain the utility of those data, as well as the structural and ecological characteristics of forest disturbances that are responsible for those constraints. Here we assess those thresholds and characteristics within the context of selective logging in the Bolivian Amazon. Our study combined field measurements of the spatial and temporal dynamics of felling gaps and skid trails ranging from <1 to 19 months following reduced-impact logging in a forest in lowland Bolivia with remote-sensing measurements from simultaneous monthly ASTER satellite overpasses. A probabilistic spectral mixture model (AutoMCU) was used to derive per-pixel fractional cover estimates of photosynthetic vegetation (PV), non-photosynthetic vegetation (NPV), and soil. Results were compared with the normalized difference in vegetation index (NDVI).

The forest studied had considerably lower basal area and harvest volumes than logged sites in the Brazilian Amazon where similar remote-sensing analyses have been performed. Nonetheless, individual felling-gap area was positively correlated with canopy openness, percentage liana coverage, rates of vegetation regrowth, and height of remnant NPV. Both liana growth and NPV occurred primarily in the crown zone of the felling gap, whereas exposed soil was limited to the trunk zone of the gap. In felling gaps >400 m^2, NDVI, and the PV and NPV fractions, were distinguishable from unlogged forest values for up to six months after logging; felling gaps <400 m^2 were distinguishable for up to three months after harvest, but we were entirely unable to distinguish skid trails from our analysis of the spectral data.

Key words: ASTER; Bolivian Amazon; felling gaps; forest disturbance; forest structure; NDVI; remote-sensing monitoring; selective logging; skid trails; spectral mixture analysis; timber harvest; tropical forest.

Introduction

Timber production in the Amazon basin has been estimated at 30×10^6 m^3/yr, based on regional sawmill production, but estimates of the areal extent and intensity of the selective logging practices that supply that timber have been poorly constrained (Nepstad et al. 1999, Lentini et al. 2003, Cochrane et al. 2004, Nepstad et al. 2004*a*). Much of the selective logging in the region is clandestine, and in many cases, legally registered forest-management plans lack credibility.

In Bolivia, illegal logging is an important cause of forest degradation in the country's lowland Amazon region (Cordero 2003). Previous timber extraction in Bolivia depleted forests of mahogany (*Swietenia macrophylla*), tropical oak (*Amburana cearensis*), tropical cedar (*Cedrela* sp.), morado (*Macherium* sp.), tarara (*Centrolobium* sp.), and tajibo (*Tabebuia sp.*) (CORDECRUZ 1994). Although recent changes in the Bolivian Forestry Law (Law 1700, 12 July 1996: Article 28) provide an exemplary framework for good forest management (Nueva ley forestal 1996, Griffith 1999), and Bolivia now has over 1.8×10^6 ha of production forests certified by the Forest Stewardship Council (FSC) (CFV 2002), the extent and intensity of logging in the Bolivian Amazon has not been quantified (Cordero 2003).

Remote sensing provides an objective means of determining the location, extent, and intensity of selective logging. Selective-logging damage, however, often occurs at a finer spatial grain than the spatial resolution of commonly available satellite imagery (Stone and Lefebvre 1998, Souza and Barreto 2000, Asner et al. 2002, Pereira et al. 2002). Furthermore, forest canopy leaf area rapidly regenerates after logging, thereby reducing the signal of indicators available via optical satellite sensors (Stone and Lefebvre 1998, Dickinson et al. 2000, Fredericksen and Licona 2000, Fredericksen and Mostacedo 2000). The study reported here was designed to improve our understanding of the

Manuscript received 13 April 2005; revised 27 September 2005; accepted 17 October 2005. Corresponding Editor: M. Friedl.
[5] Corresponding author. E-mail: djzarin@mail.ifas.ufl.edu

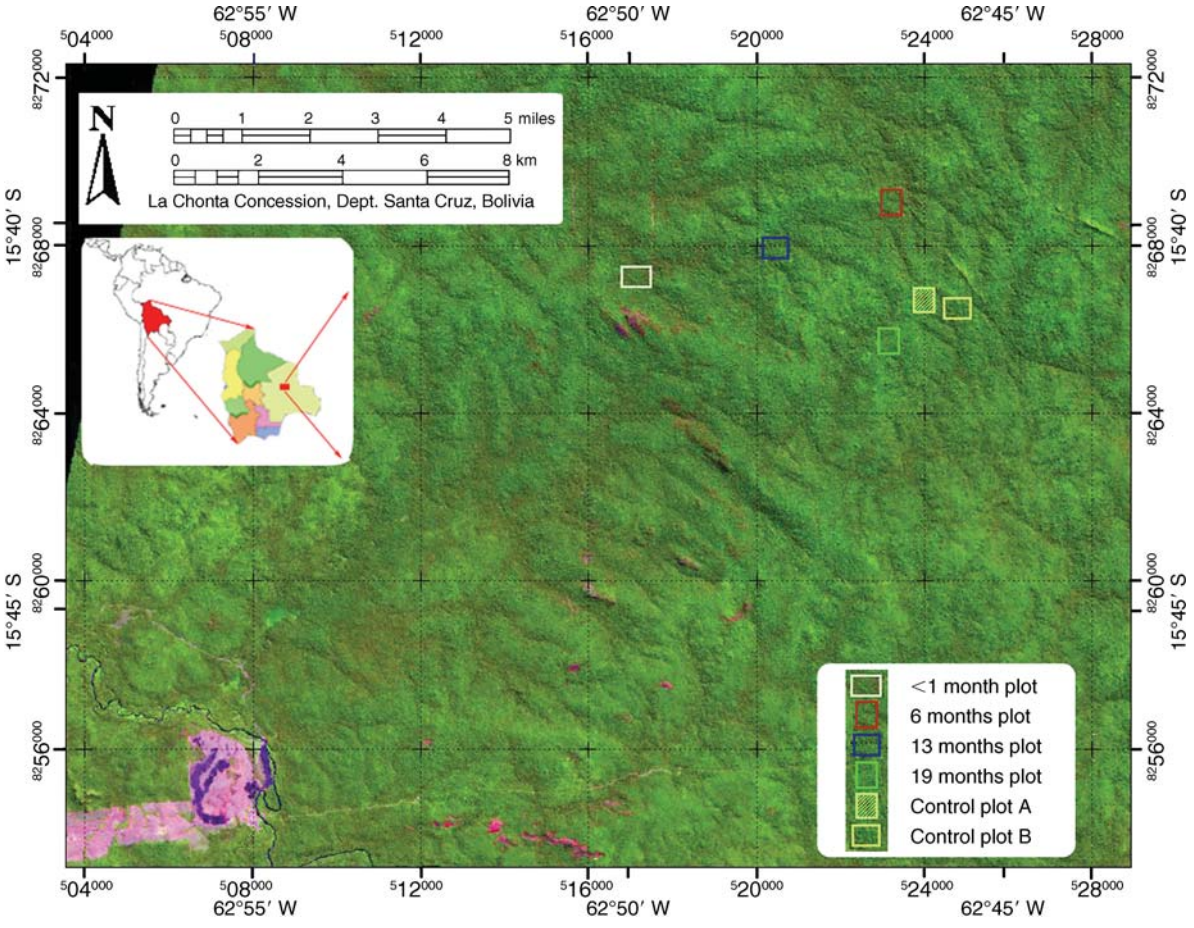

FIG. 1. Location of research plots in the La Chonta forestry concession, Department of Santa Cruz, Bolivia. The plot boundaries are overlaid on a RGB (red, green, and blue) composite image of ASTER bands 2, 3, and 1, respectively, from an image acquired on 30 June 2003. The key indicates the number of months following harvest for each of the plots. ASTER = advanced spaceborne thermal-emission radiometer.

spatial and temporal thresholds constraining the applicability of remote-sensing technology to the detection of selective logging in lowland Bolivia, and to examine the structural and ecological characteristics of logged forests that are responsible for those constraints. The specific objectives of this study were: (1) to investigate the temporal dynamics of structural and spectral properties in small, medium, and large treefall gaps and skid trails following selective logging; and (2) to evaluate the relative influence of structural and ecological characteristics measured in the field on the sensitivity of remote sensing to disturbances created by selective logging.

Previous research in the Brazilian Amazon has shown that textural and single band analysis of Landsat ETM+ (enhanced thematic mapper plus—the Landsat 7 satellite) imagery were sensitive only to high levels of canopy damage (>50% increase in canopy openness) and temporally limited to within 0.5 years postharvest (Asner et al. 2002). These techniques may have some potential for broad delineation of very recently logged forests, but they are not useful for more detailed analyses of ecological or biogeochemical processes (Asner et al. 2002). Other recent studies using spectral mixture analysis to identify exposed soil have been able to identify log decks for up to 5 years postharvest, but are unable to directly identify the forest area disturbed by logging (Souza and Barreto 2000, Monteiro et al. 2003). Asner et al. (2004*a*), employing a Monte-Carlo spectral unmixing technique (AutoMCU), were able to directly discriminate selectively logged forests in the eastern Amazon through changes in canopy openness (gap fraction), residual slash (woody debris), and exposed soil, for up to 3.5 years post-logging. The decreased canopy-gap fraction measured in the field immediately following both conventional and reduced-impact logging in 1999 and 2000 was highly correlated with canopy fractional cover derived from the spectral unmixing process 6–30 months later. The technique employed by Asner et al. (2004*a*) has been tested across a range of structural conditions and canopy-damage

conditions in the central and eastern Brazilian Amazon, but has not been applied previously to areas of diverse topographic relief, or in smaller forests and lower harvest intensities, as is typical in lowland Bolivia.

In the present study we examine the structural basis of temporal changes in spectral signatures following timber harvesting in lowland Bolivia, taking into account the potentially confounding effects of topography and seasonality by using digital elevation models and monthly ASTER imagery encompassing the wet- to dry-season transition.

Site and Methods

Site description

The study was conducted in the timber concession of Agroindustria Forestal La Chonta Ltda. The concession encompasses 100 000 ha of forest in the Guarayos province of the Department of Santa Cruz, Bolivia (Fig. 1). The elevation at the site is 400–600 m above sea level, with undulating topography. The vegetation is classified as Subtropical Moist Forest according to the Holdridge Life Zone System (Holdridge 1947), with biomass range of 73–190 Mg/ha (Dauber et al. 2000). Average tree density is 368 trees/ha, with mean basal area of 20.3 m^2/ha, mean canopy height of 25 m, and on average 59 species/ha (all data for trees >10 cm in diameter at 1.3 m height; IBIF [Instituto Boliviano de Investigacion Forestal], *unpublished data*). Common canopy trees in the area, such as *Hura crepitans, Ficus boliviana,* and *Pseudolmedia laevis*, are typical of humid forests within Bolivia (Jackson et al. 2002). Average annual temperature is 25.3°C, with mean annual precipitation of 1560 mm; 77% of the annual precipitation falls between November and April. During the dry season, temperatures often drop to 5°–10°C due to Antarctic fronts (Gil 1997). The soils are primarily moderately fertile inceptisols, with patches of black anthrosols found throughout the concession (Calla 2003, Paz 2003). The region is vulnerable to wildfires, and 30% of the concession burned in 1995 (CAF et al. 2000, Gould et al. 2002) and 2004 (C. Pinto, *personal communication*). There are ~160 tree species with individuals >10 cm in diameter at 1.3 m height within La Chonta (IBIF, *unpublished data*). Eighteen timber species are currently harvested, including *Ficus boliviana*, *Hura crepitans, Cariniana ianeirensis, Schizolobium parahyba, Ceiba pentandra,* and *Terminalia oblonga* (BOLFOR 2000).

La Chonta was certified by the Forest Stewardship Council (FSC) in 1998 and abides by certification standards, which include implementation of reduced-impact logging (RIL) techniques, such as forest inventory; mapping of harvest trees; planning of roads, log decks, and skid trails; vine cutting prior to harvest when necessary; directional felling; seed tree retention; and a 30-year cutting cycle (Johns et al. 1996, Uhl et al. 1997, Nittler and Nash 1999, Sist 2000, Pereira et al. 2002). About 70% of the concession is considered suitable for sustained-yield timber harvesting (Gil 1997), even though the concession was previously logged for mahogany (*Swietenia macrophylla*) (Gil 1997). The current annual cut is 2400 ha (Jackson et al. 2002).

Harvesting is based on a 50-cm minimum diameter at breast height (dbh) cutting limit, with the exception of *Hura crepitans* and *Ficus boliviana* that have a minimum dbh of 70 cm (Gil 1997). One year prior to harvesting, crop trees are selected, marked, and mapped, and some of the lianas in their crowns are cut (Alvira et al. 2004, Krueger 2003). Prior to harvest, skid trails are built in 150 m-intervals perpendicular to the main access road (Jackson et al. 2002). Directional felling of harvested trees reduces damage to neighboring trees, and improves ease of yarding (i.e., transporting logs from the place they are felled to a landing) (Krueger 2003). Caterpillar 518C skidders (Caterpillar, Peoria, Illinois, USA) equipped with rubber tires and winches with 15 m of steel cable are used to drag the logs to roadside log decks, where they are loaded on trucks for transport to the concession's sawmill (Krueger 2003).

Logged and control plots

Four logged plots, ranging from 27 to 31 ha, and two unlogged 27-ha control plots were used in this study (Figs. 1 and 2). Two of the logged plots, and both of the control plots, are part of the Long-Term Silvicultural Research Project (LTSRP) being carried out by the Instituto Boliviano de Investigacion Forestal (IBIF; more information *available online*)[6] in different forest types within Bolivia. All four logged plots were harvested using RIL harvesting techniques, with harvest intensities varying from 1 to 2 trees/ha (Table 1)—among the lowest found in the Amazon. Logged plots were harvested <1, 6, 13, and 19 months prior to the collection of field data in July 2003.

Replicate plots for each stage of this selective-logging chronosequence were not available. For the inferential statistical analyses described below, individual felling gaps and skid-trail segments were utilized as sample units because the structural and spectral properties we measured occur at that spatial grain, rather than at the scale of the plot as a whole (Oksanen 2001).

Plot boundaries, skid trails, and felling gaps were geolocated for the <1-mo and 6-mo postharvest plots using a global positioning system (GPS) unit (maintaining horizontal distance error <10 m with a minimum of five satellites visible) and entered into a geographic information system (GIS). The 13- and 19-mo postharvest plots had been mapped previously by IBIF researchers by creating 50 × 50 m grids over the plot area and linking skid trails and stump locations to the grid with 100-m measuring tapes. All IBIF plot maps, as well as the control-plot locations, were geo-rectified using a minimum of 15 field GPS measurements per plot collected along their periphery and interior during the summer of

[6] ⟨www.ibifbolivia.org.bo⟩

TABLE 1. Characteristics of the four selectively logged plots used in this study.

Plot (months postharvest)	Plot area (ha)	No. trees harvested	Harvest intensity (trees felled/ha)	Percentage of plot			Total gap area in overlaid gaps (%)†
				Felling gaps	Skid trails	Disturbed	
<1 month	29.7	56	1.8	8.7	4.0	12.7	3.4
6 months	27.0	27	1.0	6.9	2.4	9.3	3.1
13 months	32.0	64	2.0	10.5	5.1	15.6	6.7
19 months	28.0	29	1.0	4.2	3.8	8.0	2.9

† Overlaid gaps are defined as felling gaps in which there is more than one felled tree.

2003. The root mean-square error for the geo-located plots was consistently <5 m.

Tree-fall gaps

Tree-fall gap edges were defined by >10 m tall vegetation surrounding the ground area disturbed by the fallen tree or yarding process. The area of each felling gap was entered into the GIS using field-measured azimuth of fall from the stump (adjusted for declination). The length of the gap was measured as the longest axis. The width (minor) axis of the gap was measured perpendicular to the length (major) axis at the halfway point, and operationally the gap was defined as an oval with these two axes. Although felling-gap shapes vary, the assumption was sufficiently accurate for the questions addressed within this study, which primarily involved 30 × 30 m satellite pixels and classification within general tree-fall gap size classes. These oval polygons were geo-referenced to the geo-located stump locations. Felling gaps were classified as: small (<400 m^2), medium (400–800 m^2), or large (>800 m^2) based on their area, and were divided in half along the minor axis to form trunk and crown zones of equal size, based on analysis of the geometry of 15 random tree-fall gaps (Fig. 3). All field measurements were made separately within the two zones.

In the trunk and crown zones of each tree-fall gap separate ground surface cover estimates were made for: photosynthetic vegetation (PV); non-photosynthetic vegetation (NPV; includes trunks, branches, and senesced leaves), and exposed soil. A separate estimate of the tree-fall gap surface covered by lianas with green foliage was performed to be able to distinguish their impact from PV in general. Cover estimates were assessed visually from a height of ~5 m (obtained by standing on debris within the gap) by two independent observers; the mean of the two observations was used in the statistical analyses. In addition, the maximum height of regenerating vegetation and of woody debris (composed primarily of trunks and branches and excluding the stump) was recorded for each gap zone.

Canopy openness was estimated using a scale of 0 to 1 defined as the proportion of a standard upward-facing hemispherical mirror at 1.5 m height that has a clear view of the sky (no canopy obstruction). Canopy openness readings were taken in the middle of each gap zone (trunk and crown) along the major axis. Previous studies have shown that a canopy densiometer has comparable accuracy to digital or film hemispherical photography (Englund et al. 2000).

Felling gaps that included more than one felled tree (defined as "overlaid gaps") were identified in the GIS and removed prior to statistical analysis to avoid confounding relationships between field measurements taken in the trunk and crown felling gap zones; these overlaid gaps accounted for 3.1–6.7% of the total felling-gap area (Table 1). To analyze field data collected within the individual-tree felling gaps, a mixed three-way analysis of variance was used to test the main effects of plot (<1, 6, 13, and 19 months postharvest), size class (small, medium, and large), and gap zone (trunk vs. crown), and their interactions on canopy openness, vegetation height, NPV height, and PV, NPV, and exposed soil percentage coverage in the individual-tree felling gaps. Statistical significance of main effects provided validation for further investigation using post-hoc analyses. Tukey's and Dunnett's post-hoc tests were performed to identify significant, pair-wise differences between individual main effects within the four logged plots, and between the individual logged plots and the unlogged control forest plot, respectively.

We note that the definition of gap used in this study differs from traditional ecological measurements of gaps, which consider only areas with open canopy to be part of the gap (Brokaw 1982, Uhl et al. 1988). Because some remote-sensing systems are sensitive to ground disturbances occurring below forest canopies (Asner et al. 2004*a*), we chose to define gaps with reference to the disturbed ground area, and separately estimated canopy openness within that area. The nature of the definition of "gap" used here means that the data we report should not be compared to measurements of gaps that follow the traditional ecological convention (Brokaw 1982, Uhl et al. 1988).

Skid trails

Skid trails were sampled every 10 m in transects along straight sections. These transects ranged in length from 50 to 110 m depending on the length of the section. PV, NPV, exposed soil, and liana cover were sampled by estimating percent cover from a height of 2 m within a 2-m band perpendicular to the direction of the skid trail. Canopy openness readings were taken from those 2-m

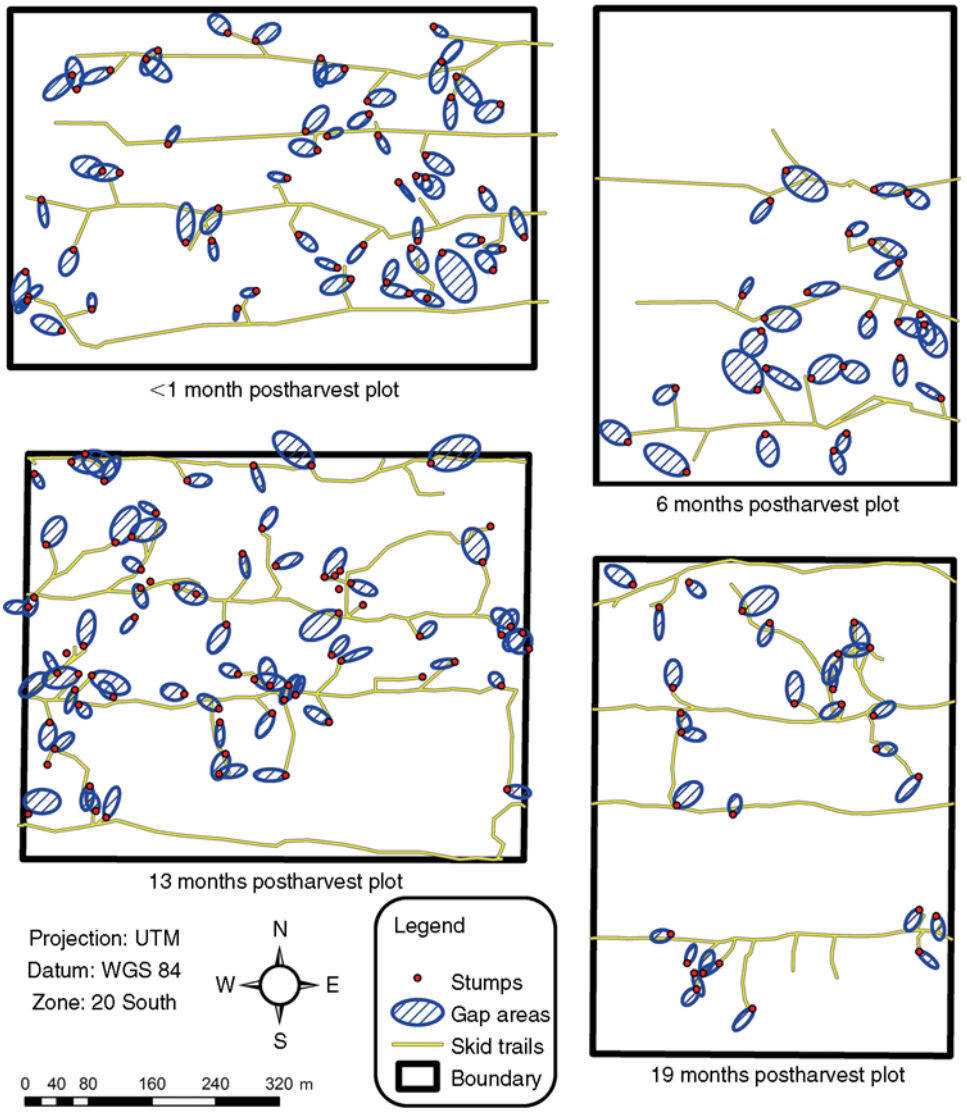

FIG. 2. Locations of tree-fall gaps and skid trails are shown for the four logged study plots in the La Chonta forestry concession. Maps of the locations of felled trees in the 13- and 19-months postharvest plots were provided by Instituto Boliviano de Investigacion Forestal (IBIF) and were used as base maps for those plots.

bands using the same methodology described for tree-fall gaps above.

A one-way ANOVA was used to test for the effect of plot on canopy openness, vegetation height, trail width, and PV, NPV, and exposed soil percent cover. Subsequently, Tukey's and Dunnett's post-hoc tests were performed to identify significant, pair-wise differences between the four logged plots, and between the individual logged plots and the unlogged control forest plot, respectively.

Skid-trail width was defined as the distance between the outer edges of the most widely separated wheel ruts. The mean width of all measurements was used to buffer the geo-referenced skid-trail centerlines to calculate per-plot skid-trail area since no significant differences (Tukey's test, $P < 0.05$) among different aged skid-trail widths existed. Skid-trail area was calculated for a total of 10, 650 × 450 m plots, including 6 additional LTSRP plots mapped previously by IBIF. Relationships between the area of skid trail and harvest intensity were investigated using a Michaelis-Menten nonlinear regression ($y = [\theta_1 x]/[\theta_2 + x]$) chosen to model the relationship based on a previous study that showed that the total area of skid trails had a positive quadratic relationship with increasing harvesting intensity (Panfil and Gullison 1998).

Control plot

A 50 × 50 m grid layout was used to establish measurement points within a 450 × 600 m unlogged control forest (Fig. 1: Control plot A); these were used for baseline comparisons. At the grid points ($n = 130$

FIG. 3. Trunk and canopy zones illustrated within a large *Ficus boliviana* treefall gap. Red arrows denote locations of zone center points. The yellow and purple lines in the gap oval represent the major and minor gap axes, respectively.

points) in the unlogged control forest, cover estimates were made from a height of 2 m within a 2-m-diameter circle placed 1 m from the edge of the path (randomly chosen as the left side) that connected the grid points.

ASTER satellite data and analyses

Advanced spaceborne thermal-emission radiometer (ASTER) images of the study area were acquired on 11 August 2001 (prior to harvest) and postharvest on 13 May 2003, 30 June 2003, 16 July 2003, and 17 August 2003 (Table 2). In this study, eight bands of spectral information were used, three covering the visible and near infrared (VNIR) *ASTER*; (bands 1–3 at 15-m spatial resolution; VNIR 0.52–.86 μm) and five covering the shortwave-infrared region (SWIR) (bands 4–8 at 30-m spatial resolution; SWIR 1.6–2.365 μm). Band 9 was not used due to noise from atmospheric water vapor. The images were preprocessed to surface reflectance (ASTER L2B product) prior to delivery, which compensated for differences in sun geometry and atmospheric conditions between the images. The surface reflectance product has been validated to within 1% and 4–7% for actual surface reflectance 15%, respectively (Abrams and Hook 2001, Yamaguchi et al. 2001). The visible-infrared (15-m pixels) images were resized to 30 m using aggregate pixel mean values and co-registered to the shortwave infrared (30-m pixels) image, then layer stacked using nearest-neighbor resampling. The use of 30-m pixels, comparable to the Landsat satellite, increases the utility of our results for subsequent applications, which will most likely utilize Landsat imagery. All images were geo-referenced using nearest-neighbor resampling to 95 ground control points (Universal Transverse Mercator [UTM], World Geodetic System 1984 [WGS 84], zone 20 south), which were acquired during the summer of 2003. The horizontal distance error (root mean square) of all geo-locations was <15 m.

We applied a probabilistic spectral mixture model using a general database encompassing the naturally occurring variability of PV, NPV, and soil spectra collected over logged and unlogged sites in the Brazilian Amazon. These spectra (termed "endmember bundles") were used to decompose the ASTER images into per-pixel estimates of photosynthetic vegetation (PV), non-photosynthetic vegetation (NPV), and exposed soil (AutoMCU; Asner et al. 2004*b*, 2005*a*) fractional cover. This model decomposed each image to sub-pixel cover fractions of PV, NPV, and soil, using the following linear equation:

$$\begin{aligned}\rho(\lambda)\text{pixel} &= \sum[C_e \times \rho(\lambda)_e] + \varepsilon \\ &= [C_{PV} \times \rho(\lambda)_{PV} + C_{NPV} \times \rho(\lambda)_{NPV} \\ &\quad + C_{soil} \times \rho(\lambda)_{soil}] + \varepsilon\end{aligned}$$

in which C is the cover fraction, $\rho(\lambda)_e$ represents the reflectance at wavelength (λ) of each endmember (e). The error term (ε) indicates the degree to which the endmembers (C_e) did not fit in the solution of multiple linear equations (one per band of spectral information per pixel) used to solve for the sub-pixel fraction of each endmember. This procedure is described in detail by Asner and Heidebrecht (2002) and Asner et al. (2004*a*, 2005*b*).

The four postharvest images were corrected for preexisting differences in topography and forest structure among the study plots by subtracting from each postharvest image the NDVI (normalized difference in vegetation index) and fractional values of the preharvest image. Potential variability between images associated with seasonality and atmospheric differences were removed by normalizing to mean NDVI, PV, NPV, and exposed-soil values present within control plots A and B (Fig. 1) in each of the five ASTER images ($n = 530$ pixels).

An ASTER digital elevation model (DEM), validated to have ≥10 m relative vertical accuracy and <50 m horizontal error (Abrams and Hook 2001) was acquired for the study area. Absolute vertical-elevation information was not crucial to this study as only relative differences in topographic shade intensity were required.

TABLE 2. ASTER image acquisition data and solar geometry.

Acquisition		Solar geometry	
Date	Time (local)†	Zenith (°)	Azimuth (°)
11 August 2001	10:33	51.49	38.22
13 May 2003	10:41	48.99	34.46
30 June 2003	10:33	44.27	32.80
16 July 2003	10:33	45.06	35.75
17 August 2003	10:33	51.49	42.31

Note: Collection zenith and azimuth angles were <15° in all acquisitions.

† All times are morning.

TABLE 3. Sample size of small, medium, and large felling gaps within the logged plots and number of pixels of treefall gaps, skid trails, and residual forest within each plot.

Plot (months postharvest)	Treefall gaps						No. skid-trail pixels	No. residual-forest pixels
	Small		Medium		Large			
	No. gaps	No. pixels	No. gaps	No. pixels	No. gaps	No. pixels		
<1 month	26 (+3)	38	27 (+11)	36	3	3	40	135
6 months	5	10	13 (+2)	22	8 (+1)	10	20	190
13 months	24 (+6)	42	14 (+12)	28	6 (+3)	12	68	127
19 months	15 (+4)	26	5 (+4)	10	1	2	57	179

Notes: Data for the number of gaps include the number of additional overlaid gaps in parentheses. Overlaid treefall gaps were not used in statistical analyses and are not included in the pixel sample sizes.

Using the DEM, Lambertian shaded-relief images (on scale of 0–100% total reflectance) were modeled based on the cosine of the sun illumination angle (elevation) and azimuth unique to each image acquisition (Table 2). Linear regressions were run between NDVI and the AutoMCU results using combined data from control plots A and B for the 16 July 2003 ASTER image ($n = 530$ pixels) and the Lambertian shaded relief values for those same pixels to estimate the influence of topographic shade. The effects of seasonality were investigated prior to normalization through the use of linear regressions between the control plot NDVI and AutoMCU values and the Julian dates (1 January is day 1) of image acquisition.

Separate two-way repeated-measures ANOVAs were used for each remote sensing variable to test the main effects of plot and image date and their interactions for small, medium, and large felling gaps, and for skid trails. Small and medium tree-fall gap sample pixels were manually selected from the images as pixels in which more than ~25% of a tree-fall gap polygon was located; in large gaps pixels were selected if they were covered more than ~50% by the tree-fall gap polygon. This approach is conservative as the sensitivity of remote sensing to tree-fall gaps could be increased by including only the most damaged pixel from each gap. Skid-trail sample pixels were selected as those that intersected with the geo-referenced skid trails in the GIS. Residual-forest (undisturbed) pixels were identified as those located within a logged plot but whose closest pixel edge was located at least 10 m from the nearest tree-fall gap or skid trail (see Table 3 for pixel sample sizes). This buffer distance was selected after analysis of 130 gridded canopy openness field measurements (every 50 × 50 m) within the 13-mo postharvest plot showed no significant relationship ($n = 130$ locations; $P > 0.05$; including all points ≥10 m from nearest disturbance) between canopy openness and distance from the nearest felling gap border or skid trail (data not shown). Asner et al. (2004*b*) showed increased canopy openness up to 50 m from felling gaps immediately following RIL; however, the majority of canopy closure occurred within the first 10 m from the gap border. Dunnett's post-hoc tests were performed to identify significant differences between the felling-gap and skid-trail pixels, and pixels located in the unlogged control plot ($n = 530$ pixels). Within the logged plots, residual-forest pixels were used to illustrate the size of the disturbance effects relative to between-plot effects. The 11 August 2003 image data of the 6-mo postharvest plot was not used because the plot had been reentered for further extraction during that month.

The 16 July 2003 image was acquired closest to the date of field data collection, so this image was used to examine the strength of relationships between the field measurements within the felling gaps and the remote-sensing responses of those same felling gaps using Pearson bivariate correlation analysis within the <1-mo and the 6-mo postharvest plots.

RESULTS

Field spatial analyses

Higher harvest intensities within the logged plots correlated with higher area in felling gaps. Felling gaps accounted for most of the disturbed area in the logged plots, ranging from 4% to 11% of the total plot area, while skid trails accounted for a maximum of 5% (Table 1). The spatial distribution of felling gaps and skid trails is illustrated in Fig. 2. Gap size ranged from 59 m^2 to 2200 m^2, and large gaps were uncommon (Table 3). The addition of data from eight other IBIF (Instituto Boliviano de Investigacion Forestal) research plots revealed a quadratic relationship between harvest

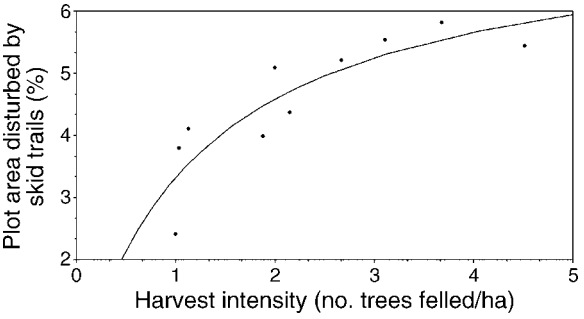

FIG. 4. Skid-trail area as a function of harvest intensity. The curve illustrates a Michaelis-Menten nonlinear model (root mean square error for the model was 0.53; estimates of θ_1 and θ_2 were 7.4 and 1.2, respectively).

TABLE 4. Results of mixed three-way ANOVAs: F statistics for the main effects of plot, gap size, and gap zone, and their interactions for variables measured in felling gaps.

Variables†	Plot	Gap size	Gap zone	Plot × gap size	Plot × gap zone	Gap size × gap zone
Canopy openness (%)	14.8***	8.6**	7.0**	1.5	0.9	4.2*
Liana coverage (%)	5.4**	0.6	31.6***	0.6	18.8***	2.3
Vegetation height (m)	11.0***	3.4*	0.3	1.8	0.5	0.5
PV coverage (%)	17.3***	0.3	13.1**	3.2**	0.1	0.2
NPV coverage (%)	7.3**	0.0	44.1***	0.8	2.8*	0.7
Soil coverage (%)	5.2**	0.7	43.0***	1.1	21.9***	2.4
NPV height (m)	6.5***	0.9	170.0***	0.7	8.8***	5.6***

*$P < 0.05$; **$P < 0.01$; ***$P < 0.001$. There were no significant three-way interactions.
† Key to abbreviations: PV, photosynthetic vegetation; NPV, non-photosynthetic vegetation.

intensity and the percentage of a plot covered by skid trails (Fig. 4).

Postharvest recovery of forest structure

Canopy openness was significantly affected by plot, size class, and gap zone, and there was a size class × gap zone interaction (Table 4). Canopy openness within felling gaps decreased significantly with time since harvest and was significantly greater for all logged plots than for the control forest (Table 5). Canopy openness within felling gaps also increased with increasing gap size (Table 6), and trunk zones had a significantly less open canopy than crown zones (Table 7). The size class × gap zone interaction reflects that canopy openness was greater in the crown zone than in trunk zone in large and medium gaps but not in small gaps (data not shown).

Liana coverage was significantly affected by plot and gap-zone effects, as well as by the plot × gap zone interaction (Table 4). Liana coverage dropped initially from the <1-mo-old to the 6-mo-old gaps, and was much higher in the older gaps (Table 5). Crown zones had significantly greater liana coverage than trunk zones (Table 7). The plot × gap zone interaction reflects that the gap-zone differences are not strongly apparent until 13 months following logging, when canopy-zone liana coverage becomes much greater than that in the trunk zone (Fig. 5a).

The height of regenerating vegetation was significantly affected by plot and gap size (Table 4), and regenerating vegetation was taller in plots that had more time to recover following logging (Table 5), and in larger gaps (Table 6).

The coverage of photosynthetic vegetation (PV) was significantly affected by plot and gap zone, as well as by the plot × size class interaction (Table 4). PV increased with time since harvest, and in the 13- and 19-months postharvest plots, PV in the gaps was not significantly different from PV in the control forest (Table 5). Crown zones had significantly less PV than trunk zones (Table 7). The interaction of plot × gap size reflects that small gaps had significantly higher PV only in the <1-month postharvest plot (data not shown).

Non-photosynthetic vegetation (NPV) was significantly impacted by plot and gap-zone processes, and by the interaction of plot × gap zone (Table 4). NPV decreased with time after harvest and was indistinguishable from the control forest in the 13- and 19-month postharvest gaps (Table 5). The crown zone had

TABLE 5. Field measurements (means with SE in parentheses) within felling gaps for <1-, 6-, 13-, and 19-months postharvest plots and within unlogged control forest.

Plot type	n†	Canopy openness (%)	Liana coverage (%)	Vegetation height (m)	Coverage (%)‡ PV	Coverage (%)‡ NPV	Coverage (%)‡ Soil	NPV height (m)
Felling gaps (months postharvest)								
<1 month	56	52.6***,a	12.8***,ac	0.6***,a	31.4***,a	49.6***,a	13.6***,a	2.6[a]
		(6.2)	(5.4)	(0.4)	(5.4)	(5.3)	(2.6)	(0.3)
6 months	26	48.7***,a	8.0***,a	1.7***,b	58.9***,b	36.6*,b	3.2[b]	2.6[a]
		(3.3)	(3.6)	(0.3)	(3.6)	(3.6)	(1.7)	(0.2)
13 months	44	26.4***,bc	24.4[c]	2.9***,c	70.8[c]	26.1[c]	3.1[b]	1.8[b]
		(2.7)	(2.8)	(0.2)	(2.8)	(2.7)	(1.3)	(0.2)
19 months	21	18.1***,c	27.1[c]	3.0***,c	79.5[c]	19.3[c]	1.3[b]	0.6
		(5.7)	(5.8)	(0.5)	(5.8)	(5.7)	(2.8)	(0.3)
Control (unlogged)	130	3.7	21.7	21.1	71.2	28.2	0.6	NS
		(0.5)	(2.4)	(1.0)	(1.7)	(1.6)	(0.3)	

Note: Different lowercase superscript letters within columns represent significant pairwise differences between logged plots (Tukey's test, $P < 0.05$). Asterisks represent significant pairwise differences between felling-gap (logged plot) and control-forest values (Dunnett's post hoc test: *$P < 0.05$; **$P < 0.01$; ***$P < 0.001$; NS = nonsignificant.
† Measured felling gaps in each age category.
‡ Key to abbreviations: PV, photosynthetic vegetation; NPV, non-photosynthetic vegetation.

TABLE 6. Field measurements (means with SE in parentheses) in small, medium, and large felling gaps, regardless of age.

Gap size	n	Canopy openness (%)	Liana coverage (%)	Vegetation height (m)	Coverage (%)			NPV height (m)
					PV	NPV	Soil	
Small	70	25.5***,a	16.3[a]	1.6***,a	61.8***,a	33.4*,a	4.0***,a	1.8[a]
		(2.3)	(2.5)	(0.2)	(2.5)	(2.4)	(1.2)	(0.1)
Medium	59	36.8***,b	15.5***,a	2.3***,b	59.3***,a	33.0***,a	5.8***,a	2.0[a]
		(2.5)	(2.4)	(0.2)	(2.4)	(2.4)	(1.2)	(0.2)
Large	18	46.8***,b	22.5[a]	2.4***,ab	59.2[a]	32.3[a]	6.1[a]	2.3[a]
		(6.2)	(5.9)	(0.5)	(5.9)	(5.8)	(2.8)	(0.4)

Notes: Different lowercase superscript letters represent significant differences between gap sizes (Tukey's test, $P < 0.05$). Asterisks represent significant pairwise differences between felling-gap and control-forest values provided in Table 5 (Dunnett's post hoc test: $*P < 0.05$; $**P < 0.01$; $***P < 0.001$). Key to abbreviations: PV, photosynthetic vegetation; NPV, non-photsynthetic vegetation; n = measured felling gaps in each size category.

significantly more NPV than the trunk zone (Table 7). The plot × gap zone interaction revealed more NPV in crown zones (vs. trunk zones) that diminished in the postharvest plot (Fig. 5b).

Soil exposure was also significantly impacted by plot and gap-zone dynamics, and by the interaction of plot × gap zone (Table 4). Soil exposure decreased with time since harvest, and only the <1-month postharvest gaps had significantly more exposed soil than the control forest (Table 5). Soil exposure was almost 20 times greater in the trunk zone than in the crown zone. The plot × gap zone interaction reflected that the differences between gap zones diminished with time postharvest (Fig. 5c).

NPV height was significantly affected by both plot and gap-zone processes, as well as by both plot × gap zone and size class × plot interactions (Table 4). NPV height decreased with increasing months postharvest (Table 5) and was higher in the crown portion of the gap (Table 7). The plot × gap zone interaction was a result of decreasing NPV height in the canopy zone, but NPV height remained the same in the trunk zone (Fig. 5d). The gap size × gap-zone interaction was a result of smaller gaps having decreased differences in NPV height between the canopy and trunk zones (data not shown).

Skid-trail PV increased with time following harvest, whereas skid-trail soil exposure decreased. Patterns were less consistent for the other variables (Table 8).

Effects of seasonality and topography on ASTER (advanced spaceborne thermal-emission radiometer) data

Both the normalized difference in vegetation index (NDVI) and the soil fraction were negatively correlated with increasing shade levels (correlation = −0.205, $R^2 = 0.015$, $P = 0.0015$ and correlation = −0.107, $R^2 = 0.064$, $P < 0.0001$, respectively) while the NPV fraction was significantly positively correlated with increasing shade levels (correlation = 0.092, $R^2 = 0.046$, $P < 0.0001$). The PV fraction, however, was not correlated with shade intensity ($P = 0.539$). Seasonality also affected the NDVI, as well as the sub-pixel fractions (PV, NPV, and soil). The NDVI and PV fractional values within the control plots declined steadily from May (early in the dry season) to mid-August (nearing the end of the dry season). Neither the NPV or soil fractions showed strong correlations ($P > 0.05$) with seasonality.

Postharvest recovery of spectral characteristics of felling gaps

Separate two-way repeated-measures ANOVAs revealed significant main effects of plot on the NDVI, and PV and NPV fractions, for small, medium, and large felling gaps. Image date was a significant main effect on the PV and soil fractions for all three gap size classes, and also on the NDVI in medium and small felling gaps. Similarly, the plot × image date interaction was a significant effect on the NDVI and PV fraction for all

TABLE 7. Field measurements (means with SE in parentheses) in trunk and canopy zones of all treefall gaps, regardless of size.

Gap zone	n†	Canopy openness (%)	Liana coverage (%)	Vegetation height (m)	Coverage (%)			NPV height (m)
					PV	NPV	Soil	
Trunk	147	33.5***,a	10.4**,a	2.0***,a	63.7[a]	24.1**,a	10.0***,a	0.8[a]
		(2.7)	(2.7)	(0.2)	(2.6)	(2.6)	(1.3)	(0.2)
Crown	147	39.3***,b	25.7**,b	2.1***,a	55.6*,b	41.8*,b	0.6[b]	3.3[b]
		(2.5)	(2.7)	(0.2)	(2.6)	(2.6)	(1.3)	(0.2)

Notes: Different lowercase superscript letters represent significant pairwise differences between gap zones (Tukey's test, $P < 0.05$). Asterisks represent significant pairwise differences between felling-gap and control-forest values provided in Table 5 (Dunnett's post hoc test: $*P < 0.05$; $**P < 0.01$; $***P < 0.001$). Key to abbreviations: PV, photosynthetic vegetation; NPV = non-photosynthetic vegetation.

† Measured trunk and crown zones.

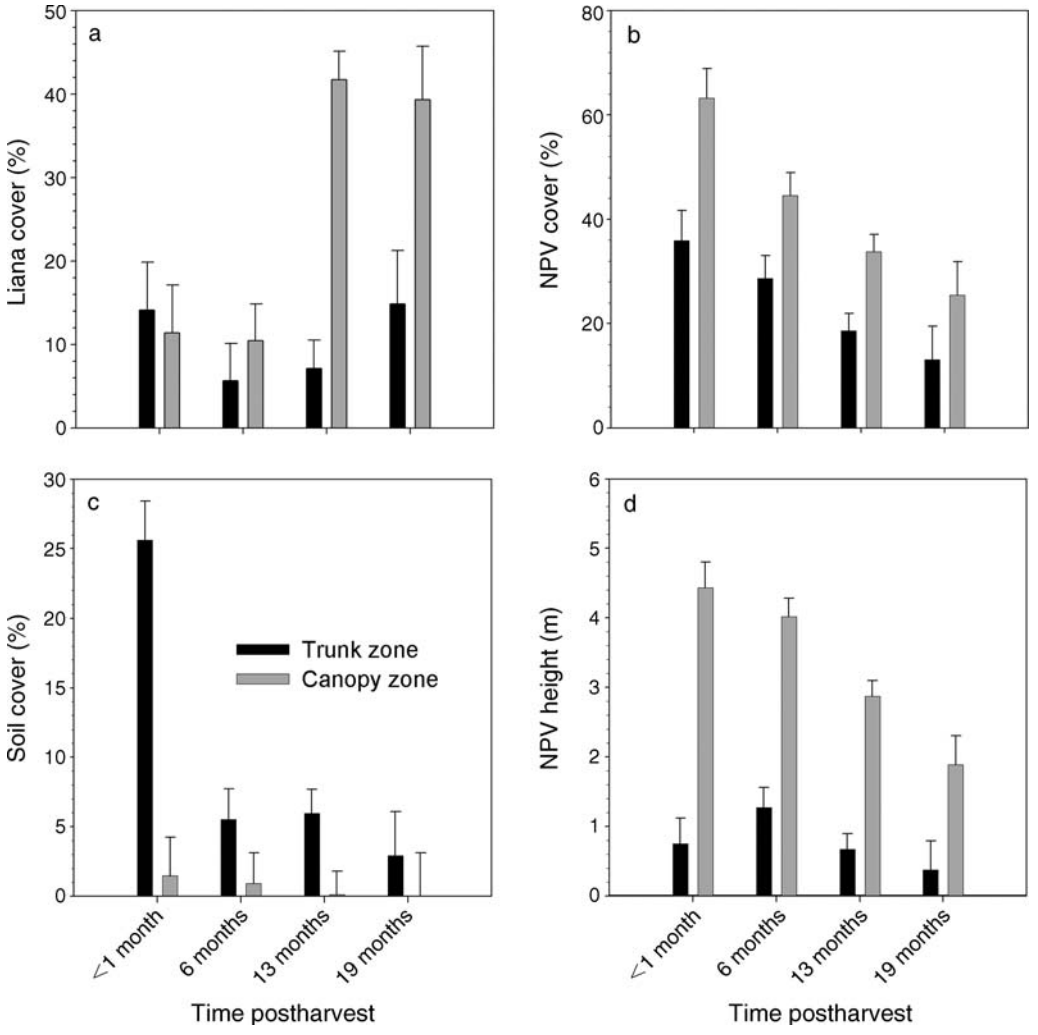

FIG. 5. Percent cover of (a) lianas, (b) NPV (non-photosynthetic vegetation fraction), (c) soil, and (d) NPV height as affected by the interaction between plot and gap zone. Data are means and SE. See Table 3 for sample sizes.

three gap size classes, and also for NPV and soil in small and medium felling gaps.

In small felling gaps (Fig. 6), the NDVI was significantly lower than for unlogged pixels only at 3 months post-logging ($P < 0.001$), but higher at 15 and 16 months postharvest ($P < 0.05$). PV was lower for 1–3 months post-logging ($P < 0.01$). NPV was higher 1 and 2 months following harvest ($P < 0.001$).

In medium-sized felling gaps (Fig. 7), the NDVI was significantly lower for up to 3 months after logging than control-plot NDVI values ($P < 0.001$). They were then higher at 13 and 15 months post-logging ($P < 0.01$). PV was lower for 1–3 months postharvest ($P < 0.01$), whereas NPV was higher 1–3 and 8 months after logging ($P < 0.05$).

In large felling gaps (Fig. 8), the NDVI was significantly lower than in unlogged control pixels for up to 3 months after harvest ($P < 0.001$), then higher at 6–8 months ($P < 0.001$) and at 16, and 20–22 months post-logging ($P < 0.05$). PV was lower for 2–3 months postharvest ($P < 0.001$) and higher at 22 months after logging ($P < 0.05$). NPV was higher 2 months post-logging ($P < 0.05$).

Linking field and remote sensing measurements

Pearson bivariate correlations between field and remote sensing measurements of all felling gaps in the <1-mo and 6-mo postharvest plots are presented in Table 9. The significant positive correlations between the NDVI and PV fraction show that, initially, they respond in a similar manner to logging disturbance, and that both are inversely correlated with NPV fraction. Soil fraction was also inversely correlated with NPV fraction. Gap area was inversely correlated with NDVI and PV fraction, and positively correlated with the PV/NPV fraction ratio in the <1-month postharvest plot, but

TABLE 8. Field measurements (means with SE in parentheses) along skid trails at four different post-logging times.

Plot (months post-logging)	Trail width			Vegetation height			Canopy openness			Coverage PV		
	(m)	*N*	*n*	(m)	*N*	*n*	(%)	*N*	*n*	(%)	*N*	*n*
<1 month	3.4[a] (0.4)	62	6	0.0***,[a] (0.1)	41	5	17.3***,[a] (16.4)	63	7	5.8***,[a] (16.3)	31	4
6 months	3.3[a] (0.3)	45	6	0.7 (0.3)***,[a]	45	6	10.1**,[a] (9.5)	45	6	18.5***,[b] (14.3)	10	1
13 months	3.4[a] (0.4)	15	2	0.3***,[a] (0.3)	15	2	5.8[b] (3.8)	15	2	NS	NS	NS
19 months	3.9[a] (0.4)	31	3	1.75***,[a] (1.2)	59	6	14.0***,[a] (14.9)	59	6	51.5***,[c] (16.2)	31	3

Notes: Different superscript letters represent significant pairwise differences between logged plots (Tukey's test, $P < 0.05$). Asterisks represent significant pairwise differences between skid-trail segments and control-forest values provided in Table 5 (Dunnett's post hoc test: $*P < 0.05$; $**P < 0.01$; $***P < 0.001$; NS = nonsignificant). Key to abbreviations: PV, photosynthetic vegetation; NPV, non-photosynthetic vegetation. *N* = number of measured locations on skid-trail transects; *n* = number of transects.

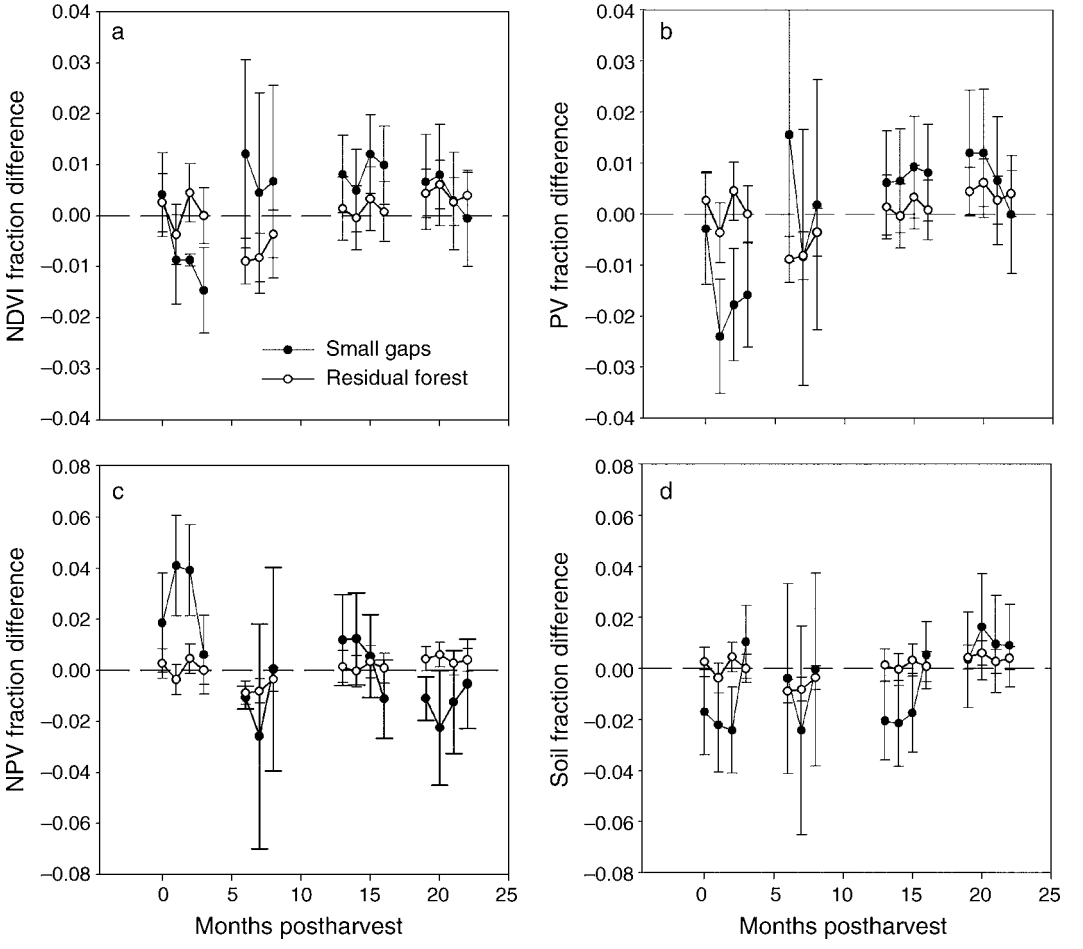

FIG. 6. Differences between spectral characteristics of small-felling-gap and unlogged-control-plot pixels for (a) NDVI (normalized difference vegetation index), (b) PV (photosynthetic vegetation), (c) NPV (non-photosynthetic vegetation), and (d) soil. Error bars are 95% confidence intervals for the small-felling-gap pixels. The differences between the treatment plot's residual-forest and unlogged-control pixels (the baseline "0.0" values) are shown to distinguish the disturbance effect from any potential effect of between-plot differences.

TABLE 8. Extended.

Coverage					
NPV			Soil		
(%)	*N*	*n*	(%)	*N*	*n*
33.6[a] (22.8)	31	3	59.5***,[a] (26.1)	31	3
47.5**,[b] (14.8)	10	1	32.0***,[b] (20.3)		
NS	NS	NS	NS	NS	NS
40.8**,[b] (17.3)	31	3	8.7***,[c] (14.6)	31	3

positively correlated only with NDVI in the 6-months postharvest plot. In the <1-month postharvest plot, canopy openness in the crown zone was also inversely correlated with the NDVI and PV fraction, and positively correlated with the PV/NPV fraction ratio. In the 6-months postharvest plot, crown-zone PV coverage was inversely correlated with the remotely sensed NPV fraction, which was positively correlated with NPV coverage. PV coverage in the trunk-zone felling gaps of the <1-month postharvest plot was correlated with the NDVI and PV fraction values, whereas NPV coverage was inversely correlated with the NDVI. NPV coverage in the trunk zone of the 6-month postharvest plot was positively correlated with NPV fraction and negatively correlated with soil fraction.

DISCUSSION

The most extensive forest disturbances resulting from selective logging are skid trails and felling gaps (Asner et al. 2004*b*). The area of forest disturbed by skid trails provides a good indicator of harvest intensity and extent for this study, but it saturates at higher harvest intensities (Fig. 4). Harvest intensity itself is more directly tied to the number of felling gaps (Pereira et

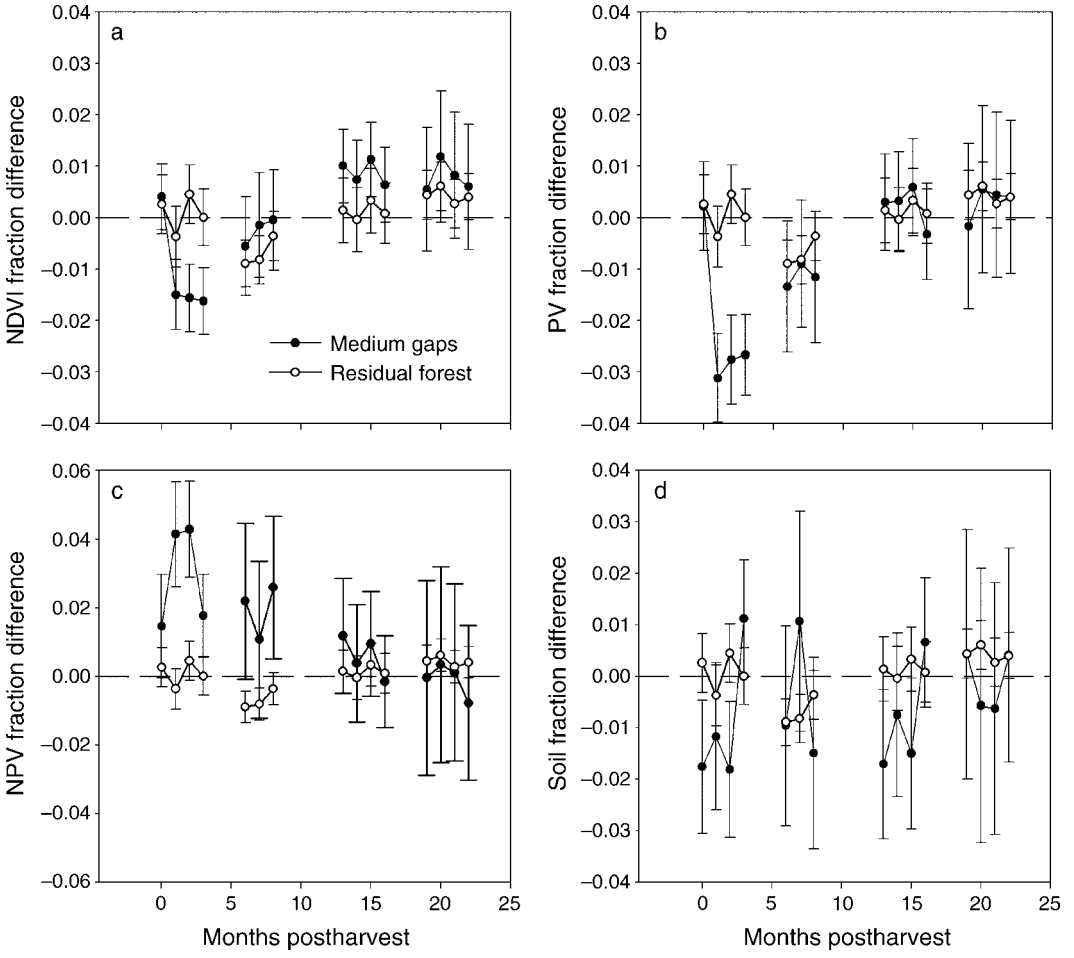

FIG. 7. Differences between spectral characteristics of medium-felling-gap and unlogged-control-plot pixels for (a) NDVI, (b) PV, (c) NPV, and (d) soil. Error bars are 95% confidence intervals for the medium-felling-gap pixels. The differences between the treatment plot's residual-forest and unlogged-control pixels (0.0 values) are shown to distinguish the disturbance effect from any potential effect of between-plot differences.

TABLE 9. Pearson bivariate correlations between field and remote-sensing measurements of felling gaps at two different post harvest times.

Felling-gap plot, <1 month postharvest					
Variable†	NDVI	PV	NPV	Soil	PV/NPV
NDVI	1				
PV	0.736***	1			
NPV	−0.450***	−0.612***	1		
Soil	NS	NS	−0.835**	1	
PV/NPV	−0.384***	−0.560***	NS	NS	1
Gap area (m^2)	−0.322**	−0.344**	NS	NS	0.553**
Gap canopy zone					
Canopy openness (%)	−0.382***	−0.311**	NS	NS	0.338**
Vegetation height (m)	NS	NS	NS	NS	NS
PV coverage (%)	NS	NS	NS	NS	NS
NPV coverage (%)	NS	NS	NS	NS	NS
Soil coverage (%)	NS	NS	NS	NS	NS
Gap trunk zone					
Canopy openness (%)	NS	NS	NS	NS	NS
Vegetation height (m)	NS	NS	NS	NS	NS
PV coverage (%)	0.316**	0.265*	NS	NS	NS
NPV coverage (%)	−0.248*	NS	NS	NS	NS
Soil coverage (%)	NS	NS	NS	NS	NS

*$P < 0.05$; **$P < 0.01$; ***$P < 0.001$; NS = nonsignificant.

† Key to abbreviations: NDVI, normalized difference in vegetation index; PV, photosynthetic vegetation fraction; NPV, non-photosynthetic vegetation fraction.

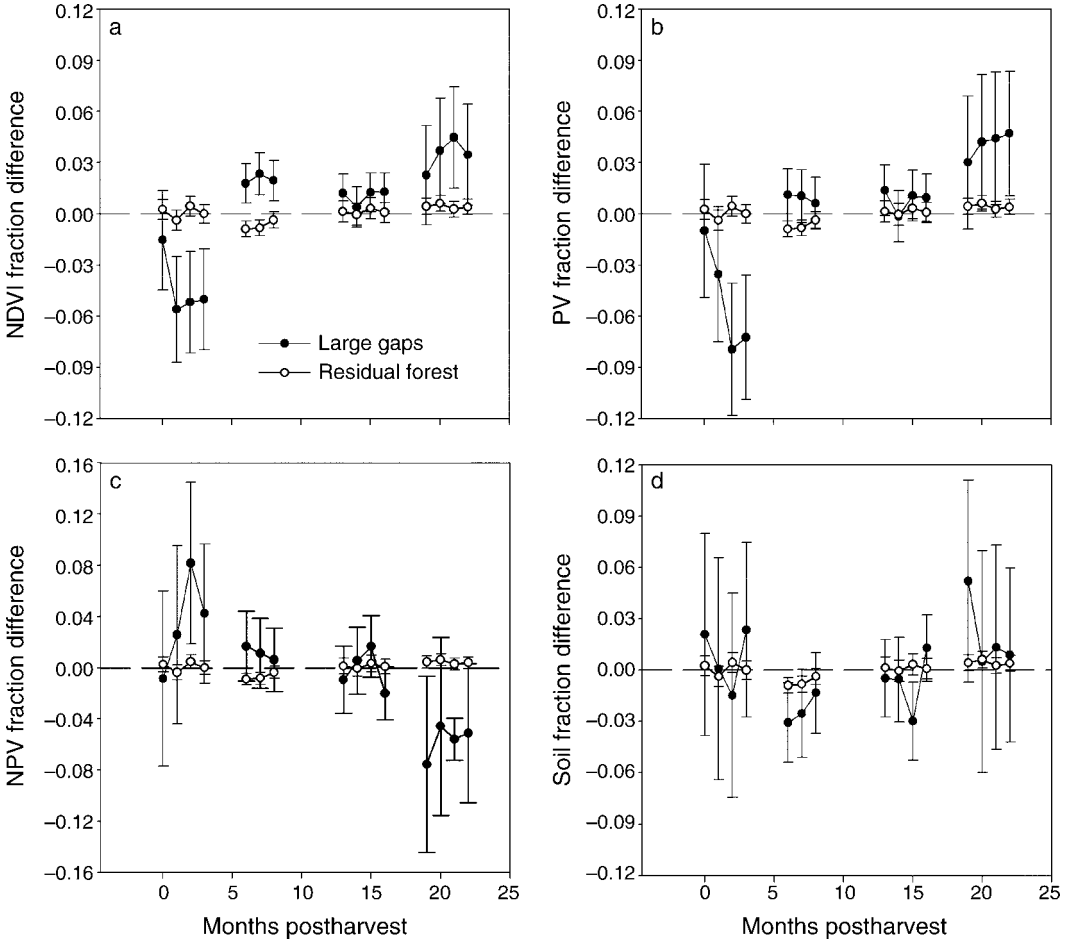

FIG. 8. Differences between spectral characteristics of large-felling-gap and unlogged- control-plot pixels for (a) NDVI, (b) PV, (c) NPV, and (d) soil. Error bars are 95% confidence intervals for the large-felling-gap pixels. The differences between the treatment plot's residual-forest and unlogged-control pixels are shown to distinguish the disturbance effect from any potential effect of between-plot differences.

TABLE 9. Extended.

Felling-gap plot, 6 months postharvest				
NDVI	PV	NPV	Soil	PV/NPV
1				
0.779***	1			
−0.526**	−0.589***	1		
NS	NS	−0.748***	1	
−0.535***	−0.737***	NS	0.622***	1
0.338*	NS	NS	NS	NS
NS	NS	NS	NS	NS
NS	NS	NS	NS	NS
NS	NS	−0.428**	NS	NS
NS	NS	0.444**	NS	NS
NS	NS	NS	NS	NS
NS	NS	NS	NS	NS
NS	NS	NS	NS	NS
NS	NS	−0.323*	NS	NS
NS	NS	0.459**	−0.371*	NS
NS	NS	NS	NS	NS

al. 2002), but that relationship may be affected by overlying felling gaps (when there is more than one felled tree). These overlaid areas, however, constituted only a small percentage of total gap area (3.1–6.7% of total plot area in felling gaps) at even the highest harvest intensities assessed in this study.

Canopy openness largely defines the ability of remote sensors to view many of the ground disturbances indicative of logging activities. The ability to distinguish felling gaps and skid trails using remote sensors has been primarily limited due to these disturbances causing only minor increases in canopy openness. This has been shown previously using both high- (Read et al. 2003) and medium- (Asner et al. 2002) spatial-resolution satellite imagery. In our study, both the normalized difference in vegetation index (NDVI) and the remotely sensed photosynthetic-vegetation (PV) fraction were significantly affected by canopy openness in tree-fall gaps <1 month postharvest.

Canopy openness generally declines from about 50–60% in felling gaps <1 month postharvest, to <20% in gaps 19 months postharvest. Rapid vegetation growth reaches 3 m in height by 19 months postharvest and covers over the soil (primarily in the trunk zone) and non-PV (NPV) (primarily in the canopy zone) exposed by logging operations. This regrowth causes the coverage of PV, NPV, and soil to change from 31%, 50%, and 14%, respectively, immediately following harvest to 80%, 19%, and 1% (respectively) after 19 months. Within that same period, rapid liana growth, concentrated in the crown zone, covers nearly 30% of the entire gap (Table 5, Fig. 5a).

Large tree-fall gaps caused substantial initial canopy damage and had increased rates of overall regeneration and rapid liana growth, as compared with small and medium gaps. This became visible via remote sensing as increased PV fraction and NDVI values after 19 months of regeneration. Rapid vegetation regrowth, coupled with the collapse of remnant NPV within the canopy zone (leaving primarily large branches and trunks above vegetation height after several months), caused large gaps to be indistinguishable by ASTER (advanced spaceborne thermal-emission radiometer) from the control forest from 6 to 16 months postharvest. Regeneration was slower in small gaps, but remained less visible in the ASTER imagery due to their smaller spatial extent, less persistent residual NPV and lower initial canopy damage. These factors were of primary importance in the most recent tree-fall gaps.

Although skid trails, which comprised 25–48% of the total disturbed area, had the highest exposed soil levels and slowest rates of vegetation recovery, they were not distinguishable from control forest with ASTER since they had relatively little impact on canopy openness. The lack of sensitivity to skid trails may also be due to the performance of the ASTER instrument, which may be more or less sensitive to changes in reflectance caused by disturbances than other instruments such as Landsat 7 ETM+ (Asner et al. 2004*a*).

In our study, large gaps, those identifiable via remote sensing for the longest time, comprised only 3–31% of all felling gaps, while medium and small gaps comprised 31–54% and 17–65%, respectively. The dominance of small and medium felling-gap sizes indicates that delineation of disturbed forested areas at a pixel level will be difficult in this context. Instead, efficient monitoring approaches will need to rely on spatial patterns among identifiable disturbed pixels to estimate the full extent of forest disturbances from logging operations. Approaches employing spatial pattern-recognition procedures to delineate logging disturbances are only recently being developed (Asner et al. 2005*a*, Souza et al. 2005). Alternative methods based on analysis of high spatial satellite imagery have potential to identify types of individual forest disturbances (Souza et al. 2003, Clark et al. 2004); however, these approaches are currently not feasible over large areas due to image availability and processing constraints.

The spectral unmixing methodology assessed in our study (Asner and Heidebrecht 2002, Asner et al. 2004*a*) shows a considerable improvement in sensitivity to lower levels of canopy damage than previous approaches (reviewed by Asner et al. 2002). Asner et al. (2004*a*), using AutoMCU-derived per-pixel PV, NPV, and soil fractions of Landsat imagery, showed sensitivity to skid trails and felling gaps, which diminished from 0.5 to 3.5 years postharvest, due to regeneration of low-stature pioneer species. Different from our results, Asner et al. (2004*a*) found that felling-gap and skid-trail PV fractions remained consistently lower than in unlogged control forest for at least two years following harvest. These differences may be a result of the higher harvest intensities in their study (2.6–6.4 vs. 1–2 trees/ha in the Brazil and Bolivia study areas, respectively), leading to

more spatially extensive canopy damage than was found in La Chonta. The higher intensities of harvest in the Brazil study area are also evident in the increased plot percentage disturbed by skid trails (2.9–8.8% vs. 2.4–5.1% in the Brazil and Bolivia study areas, respectively).

The average canopy openness and basal area in the Brazilian and Bolivian sites were similar (canopy openness of 3 ± 1% vs. 3.7 ± 5.0% [mean ± SD]) and basal area of 20–30 vs. 20.3 m^2/ha in Brazil and Bolivia, respectively); however, the average forest biomass and canopy height were greater in the Brazilian study area (average biomass of 250–300 Mg/ha (Uhl and Vieira 1989) vs. 73–190 Mg/ha and canopy height of 25–35 m vs. 25 m in Brazil and Bolivia, respectively). These differences may result in the greater and more prolonged remotely sensed differences between disturbed and intact forest areas in the Brazilian study area, with lower remotely sensed NPV and exposed soil fractions in the intact-forest areas. Finally, our study took place in an area of much greater topographic variation than did the Brazil studies, and topography has a pronounced impact on the shadowing within intact canopies and in logged areas. This presents a major confounding effect to the detection of canopy damage with remote sensing, which shows markedly decreased sensitivity to forest gaps where shadowing is more pronounced.

The results of this study increase our understanding of the utility of the ASTER satellite, and currently available remote-sensing technologies in general, for monitoring selective logging in lowland Bolivian, and identify temporal and spatial limitations. We have demonstrated that spectral unmixing methods that have been previously applied to tropical forests in the Brazilian Amazon (Asner et al. 2004*a*), where timber harvest volumes are typically higher, are also applicable to the detection of selective logging in smaller-stature forests undergoing lower intensities of harvest. Future efforts should refine the ability to distinguish logged areas from unlogged forest based on the differences from intact-forest values in sub-pixel fractional cover that are apparent in felling gaps for several months, and on the spatial distributions of felling gaps as compared with natural forest disturbances. Remote-sensing analyses that incorporate such information are only recently (Asner et al. 2005*a*) beginning to provide powerful tools for the monitoring and enforcement of forest-management regulations. An ability to monitor selective-logging activities and to accurately estimate the extent and severity of forest disturbance is also relevant for studies of carbon and nutrient cycling, preservation of faunal and floral diversity, and wildfire prevention (Nepstad et al. 1999, Pinard and Cropper 2000, Mason and Putz 2001, Keller et al. 2004, Nepstad et al. 2004*b*).

Acknowledgments

We thank M. Binford and F. Putz for valuable comments on the field and remote- sensing methodology, V. H. Lopez for assistance in collecting field measurements, BOLFOR and IBIF for field and logistical assistance, La Chonta for allowing us access to their concession and harvest information, and NASA for acquisition of the satellite imagery used for this study. This work was supported by The Florida Agricultural Experimental Station and summer research grants from BOLFOR (a forest management project of USAID and the Bolivian government), The Carnegie Institution, and NASA LBA-ECO grant NCC5-675 (LC-21).

Literature Cited

Abrams, M., and S. Hook. 2001. ASTER users handbook. Version 1. Jet Propulsion Laboratory, Pasadena, California, USA.

Alvira, D., F. Putz, and T. Fredericksen. 2004. Liana loads and post-logging liana densities after liana cutting in a lowland forest in Bolivia. Forest Ecology and Management **190**:73–86.

Asner, G., and K. Heidebrecht. 2002. Spectral unmixing of vegetation, soil, and dry carbon in arid regions: Comparing multi-spectral and hyperspectral observations. International Journal of Remote Sensing **23**:3939–3958.

Asner, G., M. Keller, R. Pereira, and J. Zweede. 2002. Remote sensing of selective logging in Amazonia: Assessing limitations based on detailed field observations, Landsat ETM+, and textural analysis. Remote Sensing of Environment **80**: 483–496.

Asner, G., M. Keller, R. Pereira, J. Zweede, and J. Silva. 2004*a*. Canopy damage and recovery after selective logging in Amazonia: field and satellite studies. Ecological Applications **14**:280–298.

Asner, G., M. Keller, and J. N. M. Silvas. 2004*b*. Spatial and temporal dynamics of forest canopy gaps following selective logging in the eastern Amazon. Global Change Biology **10**:1–19.

Asner, G., D. Knapp, E. Broadbent, P. Oliveira, M. Keller, and J. Silva. 2005*a*. Selective logging in the Brazilian Amazon. Science **310**:480–482.

Asner, G., D. Knapp, A. Cooper, M. Bustamente, and L. Olander. 2005*b*. Ecosystem structure throughout the Brazilian Amazon from Landsat data and spectral unmixing. Earth Interactions **9**:1–31.

BOLFOR [Bolivian Sustainable Forest Project]. 2000. Study plan. Long-term silvicultural research project (LTSRP) in Bolivian tropical forests. BOLFOR, Santa Cruz, Bolivia.

Brokaw, N. V. 1982. The definition of treefall gap and its effect on measures of forest dynamics. Biotropica **14**:158–160.

CAF [La Corporación Andina de Fomento], BOLFOR, and Geosystems. 2000. Bolivia: Determinación del daño causado por los incendios forestales ocurridos en los departamentos de Santa Cruz y Beni en los meses de agosto y septiembre de 1999. BOLFOR, Santa Cruz, Bolivia.

Calla, C. 2003. Arquelogía de "La Chonta." BOLFOR, Santa Cruz, Bolivia.

CFV. 2002. Consejo Boliviano para la certificación voluntaria forestal. Boletín Informativo del CFV **6**(1). CFV, Santa Cruz, Bolivia [Certificación Forestal Voluntaria].

Clark, D. B., J. M. Read, M. L. Clark, A. M. Cruz, F. M. Dotti, and D. A. Clark. 2004. Application of 1-m and 4-m resolution satellite images data to ecological studies of tropical rain forests. Ecological Applications **14**:60–74.

Cochrane, M., D. Skole, E. Matricardi, C. Barber, and W. Chomentowski. 2004. Selective logging, forest fragmentation and fire disturbance: Implications of interaction and synergy. Pages 310–320 *in* D. Zarin, J. Alavalapati, F. Putz, and M. Schmink, editors. Working forests in the Neotropics: conservation through sustainable management. Columbia University Press, New York, New York, USA.

CORDECRUZ [Corporación Regional de Desarollo de Santa Cruz]. 1994. Plan de uso del suelo (PLUS), una propuesta para el aprovechamiento sostenible de nuestros recursos naturales. CORDECRUZ, Santa Cruz, Bolivia.

Cordero, W. 2003. Control de operaciones forestales con enfasis en la actividad ilegal. Documento Tecnico 120/2003. BOLFOR, Santa Cruz, Bolivia.

Dauber, E., J. Teran, and R. Guzman. 2000. Estimaciones de biomasa y carbono en bosques naturales de Bolivia. Superintendencia Forestal, Santa Cruz, Bolivia.

Dickinson, M., D. Whigham, and S. Hermann. 2000. Tree regeneration in felling and natural treefall disturbances in a semideciduous tropical forest in Mexico. Forest Ecology and Management **134**:137–151.

Englund, S., J. O'Brien, and D. Clark. 2000. Evaluation of digital and film hemispherical photography and spherical densiometry for measuring forest light environments. Canadian Journal of Forest Resources **30**:1999–2005.

Fredericksen, T., and J. Licona. 2000. Encroachment of noncommercial tree species after selection logging in a Bolivian tropical forest. Journal of Sustainable Forestry **11**:213–223.

Fredericksen, T., and B. Mostacedo. 2000. Regeneration of timber species following selection logging in a Bolivian tropical dry forest. Forest Ecology and Management **131**:47–55.

Gil, P. 1997. Plan General de Manejo Forestal. Empresa Agroindustrial La Chonta, Santa Cruz, Bolivia.

Gould, K., T. S. Fredericksen, F. Morales, D. Kennard, F. E. Putz, B. Mostacedo, and M. Toledo. 2002. Post-fire tree regeneration in lowland Bolivia: implications for fire management. Forest Ecology and Management **165**:225–234.

Griffith, J. 1999. Resultados de los tres telleres regionales sobre la consolidacion de la ley forestal 1700. Documento Tecnico 76B. BOLFOR, Santa Cruz, Bolivia.

Holdridge, L. R. 1947. Determination of world plant formations from simple climate data. Science **105**:367–368.

Jackson, S., T. Fredericksen, and J. Malcolm. 2002. Area disturbed and residual stand damage following logging in a Bolivian tropical forest. Forest Ecology and Management **166**:271–283.

Johns, J., P. Barreto, and C. Uhl. 1996. Logging damage during planned and unplanned logging operations in the eastern Amazon. Forest Ecology and Management **89**:59–77.

Keller, M., G. Asner, N. Silva, and M. Palace. 2004. Sustainability of selective logging of upland forests in the Brazilian Amazon: carbon budgets and remote sensing as tools for evaluating logging effects. Pages 41–63 *in* D. J. Zarin, J. R. R. Alavalapati, F. E. Putz, and M. Schmink, editors. Working forests in the Neotropics: conservation through sustainable management. Columbia University Press, New York, New York, USA.

Krueger, W. 2003. Efectos del marcado de árboles de futura cosecha y la planificación de pistas de arrastre en el aprovechamiento convencional con límites diamétricos en un bosque tropical de Bolivia. BOLFOR, Santa Cruz, Bolivia.

Lentini, M., A. Verissimo, and L. Sobral. 2003. Fatos florestais da Amazonia. Imazon, Belem, Brazil.

Mason, D., and F. Putz. 2001. Reducing the impacts of tropical forestry on wildlife. Pages 473–509 *in* R. A. Fimbel, A. Grajal, and J. G. Robinson, editors. The cutting edge: Conserving wildlife in logged tropical forests. Columbia University Press, New York, New York, USA.

Monteiro, A., C. Souza, Jr., and P. Barreto. 2003. Detection of logging in Amazonian transition forests using spectral mixture models. International Journal of Remote Sensing **24**:151–159.

Nepstad, D., A. Alencar, A. C. Barros, E. Lima, E. Mendoza, C. A. Ramos, and P. Lefebvre. 2004*a*. Governing the Amazon timber industry. Pages 388–414 *in* D. J. Zarin, J. R. R. Alavalapati, F. E. Putz, and M. Schmink, editors. Working forests in the Neotropics: conservation through sustainable management. Columbia University Press, New York, New York, USA.

Nepstad, D., P. Lefebvre, U. Lopes da Silva, J. Tomasella, P. Schlesinger, L. Solorzano, P. Moutinho, D. Ray, and J. G. Benito. 2004*b*. Amazon drought and its implications for forest flammability and tree growth: a basin-wide analysis. Global Change Biology **10**:704–717.

Nepstad, D., A. Verissimo, A. Alencar, C. Nobre, L. Eirivelthon, P. Lefebvre, P. Schlesinger, C. Potter, P. Moutinho, E. Mendoza, M. Cochrane, and V. Brooks. 1999. Large-scale impoverishment of Amazonian forests by logging and fire. Nature **398**:505–508.

Nittler, J., and D. Nash. 1999. The certification model for forestry in Bolivia. Journal of Forestry **97**:32–36.

Oksanen, L. 2001. Logic of experiments in ecology: Is pseudoreplication a pseudo-issue? Oikos **94**:27–38.

Panfil, S., and R. Gullison. 1998. Short term impacts of experimental timber harvest intensity on forest structure and composition in the Chimanes Forest, Bolivia. Forest Ecology and Management **102**:235–243.

Paz, C. 2003. Forest-use history and the soils and vegetation of a lowland forest in Bolivia. Thesis. University of Florida, Gainesville, Florida, USA.

Pereira, R., J. Zweede, G. Asner, and M. Keller. 2002. Forest canopy damage and recovery in reduced-impact and conventional selective logging in eastern Para, Brazil. Forest Ecology and Management **168**:77–89.

Pinard, M., and W. Cropper. 2000. Simulated effects of logging on carbon storage in dipterocarp forest. Journal of Applied Ecology **37**:267–283.

Read, J., D. Clark, E. Venticinque, and M. Moreira. 2004. Application of merged 1-m and 4-m resolution satellite data to research and management in tropical forests. Journal of Applied Ecology **40**:592–600.

Sist, P. 2000. Reduced-impact logging in the tropics: objectives, principles, and impacts. International Forestry Review **2**:3–10.

Souza, C., and P. Barreto. 2000. An alternative approach for detecting and monitoring selectively logged forests in the Amazon. International Journal of Remote Sensing **21**:173–179.

Souza, C., Jr., D. Firestone, M. Silva, and D. Roberts. 2003. Mapping forest degradation in the Eastern Amazon from SPOT-4 through spectral mixture models. Remote Sensing of the Environment **87**:494–506.

Souza, C., Jr., D. A. Roberts, and M. A. Cochrane. 2005. Combining spectral and spatial information to map canopy damage from selective logging and forest fires. Remote Sensing of the Environment **98**:329–343.

Stone, T., and P. Lefebvre. 1998. Using multi-temporal satellite data to evaluate selective logging in Para, Brazil. International Journal of Remote Sensing **19**:2517–2526.

Uhl, C., P. Barreto, and A. Verissimo. 1997. Natural resource management in the Brazilian Amazon: An integrated research approach. BioScience **47**:160–168.

Uhl, C., K. Clark, N. Dezzeo, and P. Magurrino. 1988. Vegetation dynamics in Amazonian treefall gaps. Ecology **69**:751–763.

Uhl, C., and I. Vieira. 1989. Ecological impacts of selective logging in the Brazilian Amazon: a case study from the Paragominas region of the State of Para. Biotropica **21**:98–106.

Yamaguchi, Y., H. Fujisada, H. Tsu, I. Sata, H. Watanabe, M. Kato, M. Kudoh, A. Kahle, and M. Pniel. 2001. ASTER early image evaluation. Advances in Space Research **28**:69–76.